Unsaturated Downdraft Thermodynamics in Cumulonimbus

ALAN K. BETTS[1] AND MARIA F. SILVA DIAS[2]

Department of Atmospheric Science, Colorado State University, Fort Collins 80523

(Manuscript received 16 March 1978, in final form 21 February 1979)

ABSTRACT

The thermodynamic structure of unsaturated downdrafts driven by the evaporation of falling rain can be parameterized using an evaporation pressure scale related to downdraft speed, rain rate and raindrop population. The larger this evaporation scale, which can be inferred diagnostically from bulk downdraft data, the more unsaturated the downdraft. Simple solutions exist for constant evaporation scale in which the downdraft temperature asymptotically approaches a wet adiabat, and for buoyancy driven downdrafts where the downdraft thermodynamic paths and speed can be related to the environmental stratification. The pressure difference to the lifting condensation level for the downdraft outflow may be an observable measure of the evaporation pressure scale.

1. Introduction

The presence of unsaturated downdrafts in cumulonimbus has been known for a long time (Byers and Braham, 1949). Many authors have subsequently studied the updraft-downdraft circulations in severe storms (see Ludlam, 1963; and numerous subsequent papers). Zipser (1969) drew attention to the mesoscale unsaturated downdraft behind a tropical squall line, and subsequent papers have identified in tropical mesosystems *two* scales of downdraft: one a convective (or cell) scale and the other with the scale of the mesoscale system (Miller and Betts, 1977; Houze, 1977; Zipser, 1977; Brown, 1979). Betts (1976), while ignoring the possibility of different scales of downdraft, used the approximate conservation of equivalent potential temperature (or moist static energy) to trace the thermodynamic trajectory of unsaturated downdraft air, and to infer bulk evaporation and some features of both mixing the the vertical profile of evaporation associated with the downdraft layer outflow.

One of the GATE objectives was the determination of bulk convective parameters from aerological measurements using diagnostic models (e.g., Yanai *et al.*, 1973). Recently, these diagnostic models for cloud mass transports have included a downdraft circulation (Johnson, 1976; Nitta, 1977), although they have assumed the downdraft air to be saturated or to have a constant relative humidity. Models of this kind and cloud models for prognostic parameterization clearly need only a simple downdraft model, sufficient to describe the deviation from the dry adiabat caused by evaporation. However, it is not clear how detailed microphysical models should be averaged in time and space to give a bulk model for the thermodynamic profiles in an unsaturated downdraft. In this paper we shall take the philosophy of bulk convective parameters a stage further and explore theoretically a key bulk parameter for the downdraft structure: a *pressure scale for evaporation* of precipitation (Π_E).

We shall discuss the relationship between this evaporation scale and both the lifting condensation level (LCL) and relative humidity of downdraft outflow air, and show that at least in some conditions the LCL of cumulonimbus outflow is essentially this evaporation pressure scale. We shall also draw conclusions about the thermodynamic structure and speed of buoyancy driven downdrafts. Finally, we shall illustrate the analysis by representing downdraft thermodynamics on a tephigram and by deriving values for this evaporation scale diagnostically.

A steady-state, one-dimensional, microphysical-kinematic trajectory model, developed from Hookings (1965), Kamburova and Ludlam (1966) and Das and Subba Rao (1972), will be used to explore these constraints on downdraft structure. These papers discussed the lapse rate and relative humidity within downdrafts driven by the evaporation of falling precipitation as a function of drop size, rain intensity and downdraft speed. They showed that the stronger the downdraft speed the closer the downdraft lapse rate approaches the dry adiabat and the more unsaturated it becomes. Thus, strong downdrafts can only occur if the environmental lapse rate is close to the dry adiabat. The saturated wet adiabat can only be approached by the downdraft if the downdraft is weak, the mean drop size small and the rainfall heavy.

[1] Present address: West Pawlet, VT 05775.

[2] On leave from the Instituto Astronomico e Geofisico, Universidade de Sao Paulo, Brazil.

0022-4928/79/061061-11$06.75

Haman (1973) discussed the maintenance of downdrafts by the evaporation of cloud droplets entrained from nearby updrafts, and concluded that this mechanism might be involved in the upper and central parts of a cloud, but that the evaporation of precipitation was necessary to drive a downdraft near the ground. Studies of tropical mesosystems (Zipser, 1969, 1977; Miller and Betts, 1977; Houze, 1977) have concluded that the cell or convective-scale downdraft is driven by the evaporation of heavy rain, while the mesoscale downdraft though associated with evaporation is perhaps driven by the dynamics of the mesoscale convective system. In this paper we are concerned with constructing a thermodynamic model for a downdraft trajectory, which it is hoped may be applicable to different scales of downdraft (though for different ranges of microphysical and kinematic parameters).

2. Microphysical model

We shall extend the one-dimensional steady-state model of Kamburova and Ludlam, 1966 [discussed further in Ludlam (1979)] and cast it in a simple dimensional form [Eq. (4)].

The evaporation of a falling drop of radius r and mass m may be described by the diffusion equation

$$\left(\frac{Dm}{Dt}\right)_\nu = 4\pi r D C_v \rho (q - q_W),$$

where

- D coefficient of diffusion of water vapor in air
- C_v ventilation coefficient to allow for the motion of the drop through the air
- ρ, q air density and water vapor mixing ratio, respectively
- q_W saturation mixing ratio at the temperature of the evaporating drop, which we shall assume is the wet-bulb temperature T_W of the air.

The operator $(D/Dt)_\nu$ denotes a Lagrangian time derivative following the νth droplet. If we have a downdraft containing a population of falling evaporating drops, then we can use conservation of water to derive an equation for the change of downdraft mixing ratio with height (Kamburova and Ludlam, 1966). This conservation equation can be written (see Das, 1969 and Appendix) in Lagrangian form as

$$\rho \frac{Dq}{Dt} + \int_N d\nu \left(\frac{D}{Dt}\right)_\nu m(\nu) = 0, \tag{2}$$

where ν signifies drop number and N is the total number of drops per unit volume. This mixture of Lagrangian derivatives [one, D/Dt, following the air motion and the other, $(D/Dt)_\nu$, following the motion of the νth drop] is both necessary and helpful (Das, 1969), since the evaporation process involves a derivative following the drop motion. Substituting (1) for each drop and changing the drop spectrum variable to drop radius by defining $d\nu = n(r)dr$ gives

$$\frac{Dq}{Dt} = 4\pi D(q_W - q) \int n(r) r C_v(r) dr. \tag{3}$$

This equation describes the Lagrangian change of water vapor following an air parcel trajectory due to droplet evaporation into subsaturated air. If we neglect time and horizontal gradients of q, we obtain the change of q with pressure on a downdraft trajectory:

$$\frac{dq}{dp} = \frac{4\pi D \Delta q F}{\rho g W_D}, \tag{4}$$

where the downdraft speed W_D has been defined positive, Δq is the subsaturation $q_W - q$, and F symbolizes the integral over the drop spectrum in (3) [for a uniform drop population of N drops of size r, $F = NC_v r$]. The downdraft air will closely follow a path of constant equivalent potential temperature θ_E, although remaining unsaturated. Thus, q_W is the saturation mixing ratio at the wet-bulb temperature T_W lying on this θ_E moist adiabat, and is known. Hence if the drop spectrum integral F and downdraft speed W_D are known or assumed, (4) enables us to calculate the downdraft $q(p)$ profile, and hence $T(p)$ (since θ_E is constant) as in Kamburova and Ludlam (1966). We discuss a constraint on the downdraft speed W_D in Section 5c. The integral F is determined by the drop population, which also determines the rainfall intensity or rain flux. The details of the computational procedures using (4) will be presented later.

3. Parametric model

Clearly, we could avoid the specification of all the microphysical details in the computation of downdraft thermodynamics by specifying the combination of parameters represented by $DF/\rho W_D$. Conversely, it is this combination that can be diagnosed from bulk downdraft profile data. It is, therefore, helpful to reexpress (4) as

$$\frac{dq}{dp} = \frac{\Delta q}{\Pi_E}, \tag{5}$$

where

$$\Pi_E = \frac{\rho g W_D}{4\pi D F}. \tag{6a}$$

We may call Π_E a *pressure scale for evaporation*. Eq. (5) determines the change of mixing ratio following a downdraft trajectory due to evaporation. In this form we can regard the pressure-scale Π_E as

a bulk parameter for evaporation somewhat analogous to a pressure-scale for entrainment (see Section 5e), although Π_E is better known in terms of other parameters. Π_E is a pressure-scale not a time-scale for evaporation. Comparison of (3) which gives evaporation *rate* and (4) makes clear the role of W_D in (6a): evaporation rate has a time-scale $\Pi_E/\rho g W_D$ which is naturally independent of downdraft speed as is (1). However, the downdraft thermodynamic profiles dq/dp, $d\theta/dp$ (see below) are functions of downdraft speed, and it is these that determine the thermodynamic transformation of the atmosphere on time scales longer than that of the downdraft.

The temperature profile can be expressed in a simple analogous form. Since the downdraft θ_E follows a moist adiabat on which

$$0=\frac{1}{\theta_E}\frac{d\theta_E}{dp}=\frac{1}{\theta}\frac{d\theta}{dp}+\frac{L}{c_pT}\frac{dq}{dp}, \tag{7}$$

and at any level the wet-bulb temperature is given by

$$L\Delta q=C_p\Delta T, \tag{8}$$

where $\Delta T=T-T_W$, it follows from Eqs. (5), (7) and (8) that for the downdraft

$$\frac{T}{\theta}\frac{d\theta}{dp}=-\frac{\Delta T}{\Pi_E}$$

or

$$\frac{d\theta}{dp}=-\frac{\Delta\theta}{\Pi_E}, \tag{9}$$

where $\Delta\theta=\theta-\theta_W$, θ_W being the dry potential temperature corresponding to the wet-bulb temperature T_W.

If Π_E is known or specified, then Eqs. (5) and (9) give the change in downdraft mixing ratio and potential temperature with pressure, caused by droplets evaporating at the wet-bulb temperature. Conversely, if the downdraft thermodynamic structure is known, then one can diagnose $\Pi_E(p)$ from this one-dimensional model. Typically we find (Section 6) Π_E has a value of 20–100 mb for tropical downdrafts. The meteorological significance of these values becomes clearer if we consider the following two extremes:

$\Pi_E\to\infty$: $\dfrac{dq}{dp}, \dfrac{d\theta}{dp}\to 0$ and $\theta(p)\to$ dry adiabat,

$\Pi_E\to 0$: $\Delta q, \Delta\theta\to 0$ and $\theta(p)\to$ saturation adiabat.

The physical interpretation of (4), (5) and (6a) is straightforward. At higher downdraft speeds, Π_E is large, dq/dp is small and $d\theta/dp$ is close to the dry adiabat. Conversely, large values of the subsaturation ($\Delta q=q_W-q$) and the integral F increase dq/dp and $|d\theta/dp|$.

For a uniform population of N drops per unit volume of size r

$$\Pi_E=\frac{\rho g W_D}{4\pi DC_vNr}\propto\frac{W_D}{Nr}. \tag{6b}$$

From (6b) it would appear that as drop size increases, Π_E should decrease. However, this is misleading, since Nr is also constrained by the total liquid water content which typically has a value of a few grams per cubic meter. If we express this approximate constancy of liquid water,

$$4\pi Nr^3\rho_L/3\approx\text{constant},$$

where ρ_L is the density of liquid water, then it is clear that $1/Nr\propto r^2$, so that as the mean drop size increases, so does Π_E. This is why downdrafts remain markedly subsaturated, whereas the supersaturation in updrafts is usually negligible. Although both have comparable liquid water contents of a few grams per cubic meter, the droplet population in downdrafts consists of a far smaller number of larger droplets which evaporate less readily (see Ludlam, 1979). These larger drops also fall faster, and the integral F is perhaps more conveniently expressed in terms of rainfall rates and drop sizes (see Section 4).

4. Nomograms

Fig. 1a gives F as a function of rainfall intensity for populations of uniform drops of different sizes and a drop spectrum parameterized after Kessler (1969). We see that F increases with increasing rainfall rate and decreasing dropsize. D ($m^2\ s^{-1}$) was calculated from $0.22\ 10^{-4}\ (T_W/273.3)^{1.75}\ (1000/p)$ and C_v from $C_v(r)=1+1160r^{0.75}$, where r is in meters (see Silva Dias, 1977). Typical values are $D\approx 0.28\ 10^{-4}\ m^2\ s^{-1}$, and $C_v\approx 6.5$ at $p\approx 850$ mb in the tropical atmosphere.

Fig. 1b gives the evaporation scale Π_E as a function of downdraft speed for different values of F. We see that Π_E increases with increasing downdraft speed and decreasing F, as discussed above.

5. Some analytic simplifications

Various analytic solutions to (5) are of illustrative interest. Since $q=q_W-\Delta q$, Eq. (5) can be rewritten as

$$\frac{d}{dp}\Delta q+\frac{\Delta q}{\Pi_E}=\left(\frac{dq_W}{dq}\right)_{\theta_E}, \tag{10}$$

where we have added the suffix θ_E as a reminder that the dq_W/dp values lie on the downdraft θ_E moist adiabat.

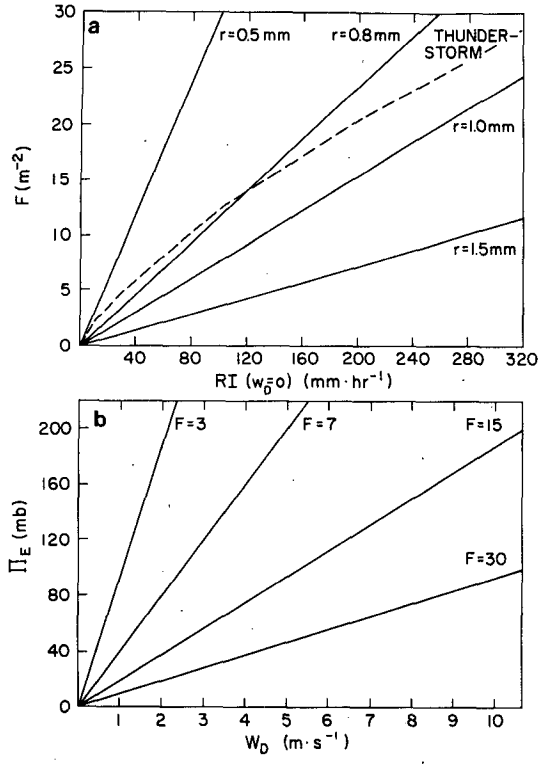

FIG. 1a. Integral $F=\int n(r)C_v(r)r^2dr$ as a function of rainfall intensity (in still air) and drop spectrum. Solid curves are for populations of uniform size drops of radius r. The dashed curve is for the Marshall-Palmer thunderstorm drop spectrum $n(r)=n_0\exp(-2\lambda r)$ using the Kessler parameterization $\lambda=4476(\mathrm{RI})^{-0.29}\ \mathrm{m}^{-1}$.

FIG. 1b. Evaporation pressure scale Π_E as a function of downdraft speed W_D and F from Fig. 1a.

a. Π_E, $(dq_W/dp)_{\theta_E}$ constant

If we take Π_E, $(dq_W/dp)_{\theta_E}$ as constants then (10) has a particularly simple and familiar solution

$$\Delta q(p)=\Delta q_I\exp[(p_I-p)/\Pi_E]+\Pi_E(dq_W/dp)_{\theta_E}\times\{1-\exp[(p_I-p)/\Pi_E]\},\quad(11)$$

where the suffix I denotes values for the inflow air to the downdraft. The initial condition Δq_I decays exponentially with pressure and Δq approaches $\Pi_E(dq_W/dp)_{\theta_E}$ asymptotically.

A transformation of (11) is particularly helpful. Referring to Fig. 2, we note that we can write in general for a linearized wet adiabat

$$\Delta q=\mathcal{P}(dq_W/dp)_{\theta_E},\quad(12a)$$

$$\Delta\theta=-\mathcal{P}(d\theta_W/dp)_{\theta_E},\quad(12b)$$

where $\mathcal{P}$ is the pressure difference to the lifting condensation level (LCL) from a pressure level p where the air has subsaturation Δq and a corresponding $\Delta\theta$. Applying (12a) to the inflow air, we can rewrite solution (11) with slight rearrangement as

$$\Delta q=\Pi_E(dq_W/dp)_{\theta_E}+(\mathcal{P}_I-\Pi_E)\times(dq_W/dp)_{\theta_E}\exp[(p_I-p)/\Pi_E)].\quad(13)$$

The first term is the asymptotic solution mentioned above, i.e.,

$$\Delta q=\Pi_E(dq_W/dp)_{\theta_E}.\quad(14)$$

By comparison with (12a) we see that in this asymptotic limit, the *pressure difference to the* LCL is the *pressure scale for evaporation* Π_E. The second term in (13) decays exponentially as p increases (i.e., downdraft parcel descends) but may also initially be smaller than the first since typically $(\mathcal{P}_I-\Pi_E)<\Pi_E$.

The solutions for $\Delta\theta$ derived from (9) are similar with an asymptotic solution

$$\Delta\theta=\Pi_E\Gamma_W,\quad(15)$$

where $\Gamma_W=-(d\theta_W/dp)_{\theta_E}$ is taken as constant. The asymptotic state given by (14) and (15) will be approached for downdraft descents $p-p_I>\Pi_E$ provided $(\mathcal{P}_I-\Pi_E)\lesssim\Pi_E$. In this asymptotic limit which follows from Π_E, $(dq_W/dp)_{\theta_E}$ and $(d\theta_W/dp)_{\theta_E}$ constant, Δq and $\Delta\theta$ become constant and the paths of both mixing ratio and temperature *parallel* the moist adiabat although the downdraft is *unsaturated* with LCL $\mathcal{P}$ equal to Π_E. We can show that this is also a state of approximately constant relative humidity.

b. Relation between relative humidity and lifting condensation level

Relative humidity (RH) is closely related to LCL. From Eq. (8) and (12), it follows using the Clausius-Clapyron equation that

$$1-\mathrm{RH}=\frac{\mathcal{P}}{q_s}(1+\gamma_A)\left(\frac{dq_W}{dp}\right)_{\theta_E},\quad(16)$$

where q_s is the saturation mixing ratio at the air temperature and γ_A is $(L/c_p)(dq_s/dT)$, the so-called psychometric "constant" for the mid-point marked A in Fig. 2. Overall, (16) is rather insensitive to temperature and only weakly to pressure. Table 1 lists corresponding values for several pressures and temperatures (though the temperature dependence is small).

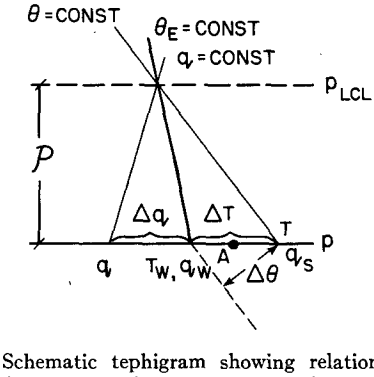

FIG. 2. Schematic tephigram showing relationship between $\Delta q=(q_W-q)$, $\Delta T=T-T_W$, $\Delta\theta=\theta-\theta_W$ and pressure difference $\mathcal{P}$ to the lifting condensation level (LCL).

Thus, the relative humidity of the downdraft outflow, which is uniquely related to the pressure difference $\mathcal{P}$ to the LCL, will also be related to the pressure scale for evaporation Π_E if the asymptotic state discussed in Section 5a is approached. The data presented later in Fig. 6 suggest that this may occur. However, another simplification of Eq. (5) is also illuminating, and may be applicable to convective-scale downdrafts through deeper layers (Section 5c).

c. Downdraft descent constrained by fixed buoyancy

In (5a), we showed that if Π_E is constant then the descent approaches an asymptote in which downdraft temperature follows a wet adiabat and Δq and relative humidity become constant. If the environmental lapse rate is between wet and dry, then this implies that the downdraft will have increasing negative buoyancy. If we assume the downdraft is buoyancy driven, then the descending air will accelerate, increasing W_D and Π_E. Since only a small temperature perturbation will generate a large W_D if the downdraft is of small horizontal scale and buoyancy driven, another useful simplification of Eq. (5) might be to suppose that the downdraft temperature path parallels the environmental lapse rate.

Substituting Eq. (5) in Eq. (7), and requiring that the downdraft $d\theta/dp=d\bar{\theta}/dp=-\bar{\Gamma}$ ($\bar{\Gamma}$ defined positive) for the mean environment, gives

$$\frac{\Delta q}{\Pi_E}=\frac{dq}{dp}=-\frac{c_pT}{L\theta}\frac{d\theta}{dp}=\frac{c_pT}{L\theta}\bar{\Gamma}. \tag{17}$$

If we take the right-hand side as constant, then dq/dp for the downdraft must be constant (and Δq and Π_E must increase or decrease together). Hence, taking $(dq_W/dp)_{\theta_E}$ also constant,

$$\Delta q=\Delta q_I+\left(\frac{dq_W}{dp}-\frac{dq}{dp}\right)(p-p_I).$$

Using Eq. (7) and (12)

$$\Delta q=\frac{c_pT}{L\theta}[\Gamma_W\mathcal{P}_I+(\Gamma_W-\bar{\Gamma})(p-p_I)]. \tag{18}$$

From Eq. (17) and (18)

$$\Pi_E=[\Gamma_W\mathcal{P}_I+(\Gamma_W-\bar{\Gamma})(p-p_I)]/\bar{\Gamma}. \tag{19}$$

From Eq. (9) and (19)

$$\Delta\theta=\Gamma_W\mathcal{P}_I+(\Gamma_W-\bar{\Gamma})(p-p_I). \tag{20}$$

From Eq. (20), (12b) and (19)

$$\mathcal{P}=\mathcal{P}_I+(\Gamma_W-\bar{\Gamma})(p-p_I)/\Gamma_W=\Pi_E\bar{\Gamma}/\Gamma_W, \tag{21}$$

showing that with this model the LCL and Π_E are in a fixed ratio. Eqs. (18)–(21) show that if $\bar{\Gamma}=\Gamma_W$ (i.e., if the environment has a wet adiabatic lapse rate) then descent with this $d\theta/dp$ will preserve $\Delta q=\Delta q_I$, and will require a $\Pi_E=\mathcal{P}_I$: this is just the asymptotic structure discussed in Section 5a. However, if $\bar{\Gamma}\neq\Gamma_W$, then the downdraft $d\theta/dp$ can only parallel the environment if Δq, $\Delta\theta$, Π_E, $\mathcal{P}$ change—linearly, with our assumption of constant gradients. Specifically, if the environmental lapse rate is between the wet and dry adiabats, $\Gamma_W-\bar{\Gamma}>0$ and Δq, $\Delta\theta$, Π_E, $\mathcal{P}$ must increase (downdraft becomes more unsaturated). Conversely, if the environment is more stable than the wet adiabat $\Gamma_W-\bar{\Gamma}<0$ and Δq, $\Delta\theta$, Π_E, $\mathcal{P}$ must decrease (downdraft moves toward saturation).

TABLE 1. Relation between RH (relative humidity) and $\mathcal{P}$ (pressure difference to LCL), for downdraft outflows exiting at different pressures and temperatures.

RH (%)	750 mb (10°C)	850 mb (15°C)	950 mb (20°C)
	←——— $\mathcal{P}$ (mb) ———→		
40	134	155	177
50	104	121	138
60	79	92	105
70	57	66	75
80	36	42	48
90	18	20	23

This is of great significance. In the first case, the downdraft "dries out," and this imposes no constraint on further evaporation. In the second, descent may be limited because the downdraft *must* move toward saturation in order to follow the rather stable environmental lapse rate. If saturation is reached at pressure p_S when $\Delta\theta=\Delta q=\Pi_E=\mathcal{P}=0$, Eqs. (18)–(21) show that the descent

$$(p_S-p_I)=\mathcal{P}_I\Gamma_W/(\bar{\Gamma}-\Gamma_W). \tag{22}$$

In the tropical atmosphere $\bar{\Gamma}-\Gamma_W$ typically becomes positive above the mid-troposphere (~600 mb), where $\bar{\theta}_{ES}$ has a minimum, so that Eq. (22) suggests that downdrafts from the upper troposphere may not be favored. We also can interpret Eq. (22) in terms of the environment gradient of saturation equivalent potential temperature θ_{ES}, i.e.,

$$\frac{d\bar{\theta}_{ES}}{dp}\approx(1+\gamma)\frac{\bar{\theta}_{ES}}{\bar{\theta}}(\Gamma_W-\bar{\Gamma}), \tag{23}$$

so that the gradient of $\bar{\theta}_{ES}$ reverses sign and $\bar{\theta}_{ES}$ has a minimum where $(\Gamma_W-\bar{\Gamma})$ goes from positive to negative. Since the downdraft conserves θ_E, then we might generally conclude that air from above this $\bar{\theta}_{ES}$ minimum cannot descend through this level (in a buoyancy driven downdraft) if it has $\theta_E>\bar{\theta}_{ES}$ (min).

Finally, we may draw conclusions about the variation of downdraft speed W_D from the variation of Π_E necessary if the downdraft temperature parallels that of the environment. From Eq. (6) we see that Π_E is

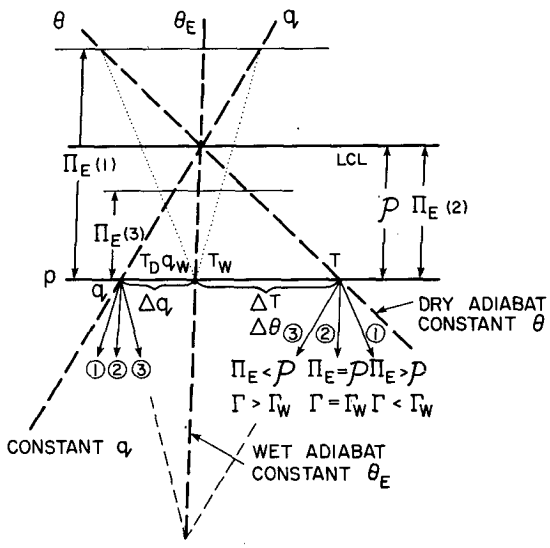

FIG. 3. Schematic tephigram showing initial downdraft descent paths (thin solid lines) for different magnitudes of evaporation scale $\Pi_E(>\mathcal{P}, =\mathcal{P}, <\mathcal{P})$, labeled ①, ② and ③, respectively. Paths ③ for small Π_E intersect at saturation on wet adiabat if projected (light dashed lines), as do lines ① if projected back (not shown). Light dotted lines are construction lines parallel to descent paths ① with slopes $\Delta q/\Pi_E$①, $\Delta\theta/\Pi_E$①. Π_E③ is shown, but construction lines for paths ③ are omitted.

essentially related to W_D and F which in turn can be related to rainfall intensity (Fig. 1). If we regard the rainfall intensity at a given location in a storm as given by the structure of the storm and the stage in its life cycle and to be only a weak function of height, then large variations in Π_E with pressure clearly must be attributed to the variation of W_D. That is, the linear downdraft increase in Π_E given by Eq. (17) for $\Gamma_W > \bar{\Gamma}$ can be interpreted (since rain flux and F vary only weakly with height) as a linear increase in speed W_D. This increase is necessary to reduce the magnitude of dq/dp, $d\theta/dp$ so that downdraft temperature can follow the environment Γ rather than the wet adiabat. Conversely, if $(\Gamma_W - \bar{\Gamma}) < 0$ (a very stable atmosphere), the decrease of Π_E may be interpreted as a decrease in W_D, until the descent finally stops as the air becomes saturated and could only descend following the saturation adiabat.

As was argued at the beginning of this subsection, changes in W_D can be produced by small changes in buoyancy, so that the assumption $d\theta/dp = d\bar{\theta}/dp$ is still an excellent approximation in Eq. (17). If we set $W_D = R\Pi_E$, where R symbolizes a microphysical parameter (e.g., the slope of lines in Fig. 1b), then from Eq. (19)

$$W_D = R[\Gamma_W \mathcal{P}_I + (p - p_I)(\Gamma_W - \bar{\Gamma})]/\bar{\Gamma}. \qquad (24)$$

This equation predicts that downdraft speed will increase with the dryness of the inflow ($\mathcal{P}_I$ large), with the instability of the environment (as $\bar{\Gamma} \to$ dry adiabat, $\Gamma_W - \bar{\Gamma}$ increases and $\bar{\Gamma}$ decreases toward zero), and with descent ($p - p_I$ increasing). Of course, once the influence of the surface is felt strongly through the nonhydrostatic pressure field, W_D must decrease and the downdraft $d\theta/dp$ depart (on the cooler side) from the assumed $\bar{\Gamma}$.

Although this fixed buoyancy analysis is illuminating, its range of applicability is unclear. The complex three-dimensional structure of mesoscale precipitating storms often makes an "environment" hard to define even for convective-scale downdrafts, and the neglect of the perturbation pressure field becomes an increasingly invalid approximation as one moves towards the mesoscale (~10 km).

There is some evidence that a few intense downdrafts in midlatitudes, called downbursts by Fujita and Byers (1977), do not slow down until within a hundred meters or so of the ground. Fujita and Caracena (1977) also suggest that downdrafts can originate in the upper troposphere beneath the collapsing tops of cumulonimbi. In intense thunderstorms the weight of liquid water may be an important contribution to negative buoyancy. In addition, if the lower troposphere is very unstable and hence favorable to strong downdrafts, this potential energy source might be sufficient to drive downdrafts through the deep troposphere (through the nonhydrostatic pressure field). Although both these effects have been neglected in the derivation of (22), it still seems unlikely that downdraft air that reaches near the surface can *originate* much above the level of minimum $\bar{\theta}_{ES}$. It is more likely that heavy precipitation beneath collapsing cumulonimbus tops drives the low-level strong downdraft from the middle troposphere.

d. Tephigram representation

We can summarize this section on a thermodynamic diagram. Fig. 3 starts with downdraft air with properties T, T_W, T_D at a certain pressure level, with a corresponding lifting condensation level $\mathcal{P}$ (mb) above. Three subsequent descent paths ①, ②, ③ are shown all of which involve evaporation but conserve equivalent potential temperature (clearly, if there were no evaporation, the descent would follow the dashed lines of constant θ, q). If the evaporation pressure scale $\Pi_E > \mathcal{P}$ then the descent path follows ① (between the wet and dry adiabats for the temperature path). Thus, Δq, $\mathcal{P}$ will increase, and this path can only continue to be followed if Π_E also increases [as in Eq. (19)]. If, however, we have a state where $\Pi_E = \mathcal{P}$, then the temperature descent path ② follows a wet adiabat and Δq, $\Delta\theta$, the relative humidity and $\mathcal{P}$ remain constant. This is the asymptotic state (for constant Π_E) discussed in Section 5a. If $\Pi_E < \mathcal{P}$, then the temperature descent path ③ is more stable than the wet adiabat, and Δq, $\Delta\theta$, $\mathcal{P}$ decrease, while relative humidity increases, heading toward saturation. Saturation can only be reached if Π_E also keeps decreasing

($<\mathcal{P}$) toward zero. Realistically this can only happen if the downdraft slows down, since the rainfall rate cannot increase without limit, as discussed in Section 5c.

One method (of several) for constructing the instantaneous downdraft path given Π_E is shown as dotted lines connecting the wet-bulb temperature to the dry adiabat and constant q line at a level Π_E above. These dotted lines are parallel to the desired downdraft paths (1) since $dq/dp=\Delta q/\Pi_E$ and $d\theta/dp=-\Delta\theta/\Pi_E$. Although not shown on the diagram for clarity, it should be noted that paths marked ①, if projected backward, also intersect at a point on the θ_E moist adiabat (if the curvature of the θ_E line is neglected) as given by Eq. (22).

e. *Entrainment into a downdraft*

One can extend (5) to include entrainment of dry air into a downdraft. Let ω^*, q be the downdraft mass flux and mixing ratio and neglect "detrainment" of downdraft air. Then

$$\frac{d}{dp}(\omega^* q)=\omega^*\frac{\Delta q}{\Pi_E}+\frac{d\omega^*}{dp}\tilde{q}, \tag{25}$$

where $\tilde{q}$ is the mixing ratio of the entrained air (assumed "environment"). This equation describes the change of the downdraft *vapor* mixing ratio by dilution and evaporation. The precipitation drop spectrum and rainfall rate will also be affected by the entrainment process, resulting in a change in Π_E with pressure. This we shall not attempt to determine. Eq. (25) can be rewritten as

$$\frac{dq}{dp}=\frac{q_W-q}{\Pi_E}+\frac{\tilde{q}-q}{L_e}, \tag{26}$$

where $L_e=(1/\omega^*)d\omega^*/dp$ is a pressure scale for entrainment. Thus, the downdraft mixing ratio changes by two processes: evaporation of drops at the wet-bulb saturation mixing ratio q_W (with a scale Π_E) and entrainment of air with mixing ratio $\tilde{q}$ (with scale L_e).

6. Some diagnostic results

Betts (1976) inferred downdraft inflow and outflow properties assuming conservation of θ_E, using soundings before and after mesoscale convective systems over Venezuela. We shall use this data to illustrate the analysis and add a few data points from the GARP Atlantic Tropical Experiment, also from inferred trajectories. Additional assumption, however, are necessary since the inferred trajectories only give inflow and outflow data rather than a vertical profile in the downdraft. These end point data roughly imply a mean value of Π_E but the detailed structure $\Pi_E(p)$ cannot be uniquely determined. Π_E itself is a combination of microphysical parameters and downdraft speed [Eq. (6)] so that an inferred trajectory corresponds to a large family of conditions. These conditions comprise the downdraft mass flux ρW_D, and the drop spectrum which determines F and the rainfall rate in still air. The procedure we shall follow to determine this family of conditions is to specify the shape of the downdraft mass flux and the form of the drop spectrum. In the data presented here we shall take ρW_D independent of pressure, and we shall consider populations of uniform size drops, and a drop spectrum [parameterized after Kessler (1969)].

a. *Computational procedure*

The procedure is iterative. A value of ρW_D is specified, together with an initial rain rate, and the trajectory of $q(p)$, $\theta(p)$ is computed stepwise for the downdraft using (4) and the equations given below. The initial rain rate is raised until the outflow data are matched. A new value of ρW_D can then be chosen and the calculation repeated.

For a uniform drop population the computation follows Kamburova and Ludlam (1966). Rainfall rate (RI) is related to rain density ρ_R according to

$$\mathrm{RI}=\rho_R(V_T+W_D), \tag{27}$$

where the rain density (kg m^{-3}) is

$$\rho_R=\tfrac{4}{3}\pi N r^3\rho_L. \tag{28}$$

The terminal velocity is given by (Manton and Cotton, 1977)

$$V_T=2.13\left(\frac{\rho_L}{\rho}gr\right)^{\frac{1}{2}}, \tag{29}$$

where ρ_L is the density of liquid water. Eq. (28) gives an initial value of the drop number N per unit volume. An initial value of F can be computed and Eq. (4) then used to find dq/dp and hence $q(p+\Delta p)$. Conservation of θ_E gives a corresponding $T(p+\Delta p)$. The expressions for C_v and D were given in Section 4. The change of N with pressure is found from conservation of drop number, i.e.,

$$\frac{d}{dp}[N(V_T+W_D)]=0. \tag{30}$$

The change in rain density (and rain flux) is correspondingly found from conservation of water. Eq. (2) becomes

$$\frac{d}{dp}[\rho q W_D+\rho_R(V_T+W_D)]=0. \tag{31}$$

A new value of ρ_R and N is used to compute the new drop radius, and the computation of dq/dp is repeated with new values.

For a drop spectrum, Kessler's (1969) parameteriza-

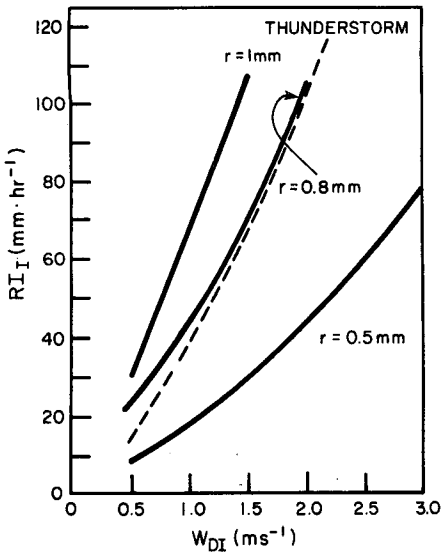

FIG. 4. Family of initial conditions (initial rainfall rate RI_I, downdraft speed W_{DI}) diagnosed from end points of a mean Venezuelan downdraft trajectory (assuming constant mass flux ρW_D) for different uniform drop sizes (solid curves) and a continuous thunderstorm drop spectrum (as in Fig. 1).

tion is used. This uses a Marshall-Palmer spectrum

$$n(r)=n_0\exp(-2\lambda r), \tag{32}$$

where

$$n_0=1.6\times 10^7,$$
$$\lambda=b[\mathrm{RI}(W_D=0)]^\beta=b(\rho_R\bar{V}_T)^\beta.$$

The parameters b and β are related to rainfall type, and we shall use thunderstorm parameters $b=4476$ m^{-1}, $\beta=-0.29$ (from Mason, 1971).

A mean terminal velocity $\bar{V}_T$ is used given by

$$\bar{V}_T=1.94V_T(r_m),$$

where

$$r_m=\lambda/2.$$

In this drop spectrum case (32) is used to compute $n(r)$ from ρ_R and hence F in (4). Eq. (31) with a mean $\bar{V}_T$ gives the change of ρ_R from dq/dp and hence a new spectrum using (32) again.

b. Results

Fig. 4 shows the family of initial downdraft speeds (ρW_D was kept constant) and initial rainfall rates which match the inflow and outflow parameters for the mean downdraft trajectory for the Venezuelan systems in Betts (1976). Three drop sizes (uniform drops with radius $r=0.5$, 0.8 and 1.0 mm) and a continuous thunderstorm drop population are shown. These curves correspond to the ranges of physical conditions which would produce the observed (mean) downdraft outflow in T, q and θ_E from the inflow for the different drop populations. However, even if we accept the thunderstorm drop distribution we cannot tell without further information whether the downdraft air descended in a moderately fast downdraft in heavy rain ($W_D\approx 2$ m s^{-1}, rainfall intensity RI ≈ 100 mm h^{-1}) or more slowly in light rain. Nevertheless, it is apparent that in these tropical storms where measured rainfall intensities are typically <200 mm h^{-1} over 5 min periods that corresponding downdraft velocities averaged over the descent are less than a few meters per second. It is also apparent that a model with a single drop size may be as useful as a drop spectrum model for some diagnostic purposes.

It is straightforward to compute Π_E from (6) for the families of downdraft parameters. Fig. 5 shows that the curves of Fig. 4 collapse into almost one curve for Π_E. Larger drop sizes and rainfall rates are well represented by the solid curves; only for small drop sizes and corresponding low rainfall rates and downdraft speeds (example for Π_E shown dashed) do the curves diverge a little. Once we take ρW_D constant, Π_E varies only slightly with pressure (D decreases by about 12% and F by 0–20% as the rainfall rate decreases).

We may conclude that once constant ρW_D is assumed, the downdraft trajectory is essentially characterized by a vertically averaged pressure scale $\bar{\Pi}_E$. Furthermore, even different assumptions of ρW_D do not change $\bar{\Pi}_E$ by much (although they do change the inferred vertical profiles of Π_E, Δq), since the

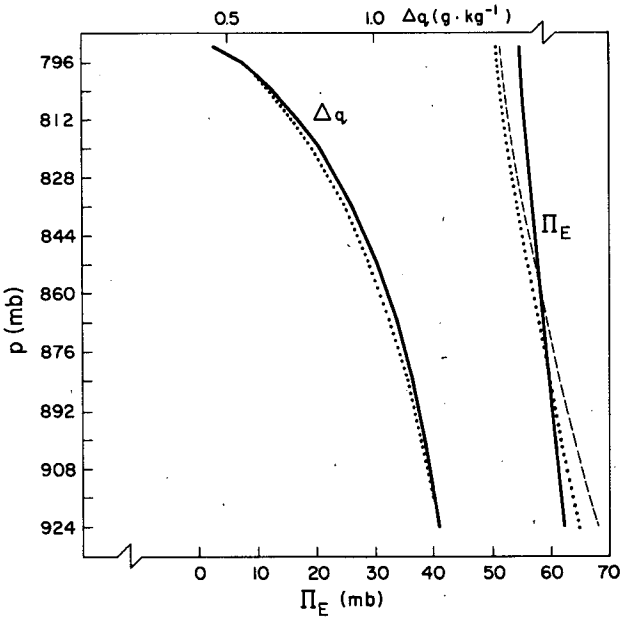

FIG. 5. Diagnosed pressure scale $\Pi_E(p)$ and $\Delta q(p)$ corresponding to some of the family of curves in Fig. 4. The Δq curve is almost independent of downdraft speed and microphysics: the solid curve is for $RI_I=140$ mm h^{-1}, $W_{DI}=2.5$ m s^{-1}, $r=0.8$ mm; the dotted curve is for the thunderstorm drop spectrum [$RI_I=64$ mm h^{-1}, $W_{DI}=1.5$ m s^{-1}, $\lambda=4476$ (RI)$^{-0.29}$ m]. Three Π_E curves are shown: the third (dashed) is for $RI_I=9$ mm h^{-1}; $W_D=0.5$ m s^{-1}, $r=0.5$ mm). The solid curves are representative of all large rainfall rates.

TABLE 2. Layer-averaged parameters for 24 sounding pairs (and their mean) considered representative of downdraft inflow and outflow for VIMHEX.

	Inflow					Outflow				
Sounding no.	p_I (mb)	T_I (°C)	q_I (g kg^{-1})	θ_{EI} (K)		Sounding no.	p_0 (mb)	T_0 (°C)	q_0 (g kg^{-1})	θ_{E0} (K)
Mean	792	13.9	11.3	340.8		Mean	924	21.4	13.4	340.5
59	855	17.6	13.6	344.4		60	945	21.9	15.3	344.4
59	870	18.5	14.2	345.5		61	950	21.8	15.9	345.5
81	735	10.9	9.5	339.2		82	905	21.2	12.2	338.9
81	720	8.9	9.5	338.8		83	900	20.4	12.2	338.5
100	810	15.2	12.7	344.2		101	930	20.9	15.0	343.9
100	765	11.9	8.9	334.7		102	915	20.3	11.9	335.9
116	825	17.0	11.9	342.2		117	935	23.0	13.8	342.4
120	765	13.2	10.9	342.2		121	915	20.6	14.2	342.9
120	930	24.4	15.7	350.2		122	970	23.7	17.5	350.3
120	825	17.2	13.3	346.6		123	935	23.1	15.3	346.9
131	870	18.6	14.2	345.6		132	950	23.9	15.2	346.0
131	840	17.0	13.0	343.7		133	940	23.1	14.5	344.0
176	735	10.7	9.5	339.0		177	905	18.6	13.4	339.3
176	870	20.7	13.5	346.1		178	950	22.5	15.7	345.7
192	795	14.0	11.4	340.8		193	925	21.2	13.8	341.3
192	855	18.0	13.8	345.4		194	945	22.4	15.5	345.6
203	765	12.3	8.8	334.9		204	915	19.9	11.8	335.1
226	840	17.7	11.5	340.1		228	940	22.0	13.5	339.8
241	735	10.5	9.1	337.5		242	905	21.2	12.0	338.3
241	735	10.5	9.1	337.5		243	805	19.9	12.5	338.2
312	750	11.7	10.0	339.7		317	910	18.4	13.6	339.1
312	705	9.1	7.9	336.3		318	895	19.2	11.7	336.2
324	735	9.8	9.1	336.7		325	905	18.1	12.8	337.0
324	840	16.6	13.0	343.2		326	940	23.7	14.1	343.6

end points of the trajectory (the downdraft inflow and outflow properties) are fixed.

The computation of a downdraft trajectory Π_E and a vertical average $\bar{\Pi}_E$ was repeated (assuming ρW_D constant) for individual sounding pairs. The data set were the Venezuelan convective systems in Betts (1976) (which are in the average used above) and two GATE squall lines. Table 2 shows the sounding pairs considered representative of inflow and outflow for the Venezuelan data. The inflow sounding is used independently in each of the sounding pairs with a different outflow sounding. The selection of bulk layer averages was the same as that in Betts (1976). For the GATE sounding pairs a simpler procedure was used to estimate layer-averaged downdraft inflow and outflow properties (Table 3). A 100 mb layer above the surface was averaged and considered representative of the downdraft outflow air and a search was made of the sounding considered representative of the inflow for a 100 mb layer with the same average θ_E.

Figs. 6a and 6b show plots of $\bar{\Pi}_E$ against the LCL for the downdraft inflow $\mathcal{P}_I$ and outflow $\mathcal{P}_0$. Fig. 6a shows no correlation, but Fig. 6b shows that the outflow LCL is correlated quite well with the mean evaporation scale, suggesting that the asymptotic state (Section 5a) has been approached in most cases. The wide variation in the values of $\bar{\Pi}_E$, $\mathcal{P}$ from different storms and rawinsonde pairs indicate either variations in downdraft processes or inhomogeneities in the atmosphere which present a sampling problem of the rawinsonde.

If the outflow $\mathcal{P}_0 \approx \bar{\Pi}_E$, then the total evaporation during the downdraft descent from $\mathcal{P}_I$ to $\mathcal{P}_0$ can be written as

$$q_0 - q_I \approx \left(\frac{dq_W}{dp}\right)_{\theta_E} (\mathcal{P}_I - \bar{\Pi}_E + p_0 - p_I) \qquad (33)$$

if approximate constancy of $(dq_W/dp)_{\theta_E}$ is assumed as in Section 5. The dependence on the descent dis-

TABLE 3. As in Table 2 but for the GATE squall lines.

		Inflow					Outflow				
Ship	Day	Time	p_I	T_I	q_I	θ_{EI}	Time	p_0	T_0	q_0	θ_{E0}
Oceanographer	11 Sep	1801	763	11.0	9.5	335.7	2216	963	19.5	13.7	335.1
Dallas	12 Sep	0908	738	8.8	9.2	335.6	1800	963	23.0	12.7	336.4
Oceanographer	12 Sep	1215	775	10.9	9.6	334.4	1513	963	22.6	12.2	334.5
Research	12 Sep	1154	863	16.8	12.0	337.8	1902	963	21.7	13.5	337.1

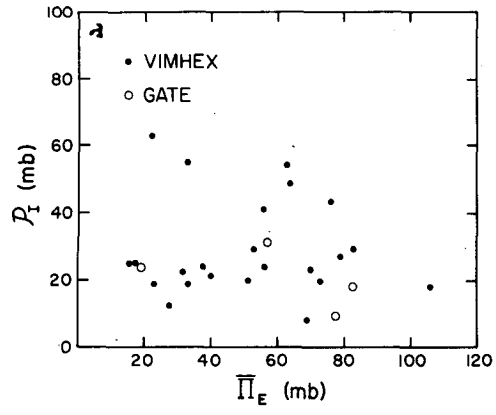

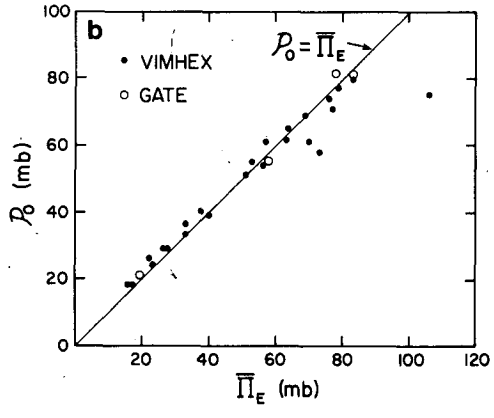

FIG. 6a. Mean evaporation scale $\overline{\Pi}_E$ vs inflow lifting condensation level $\mathcal{P}_I$, showing no correlation.

FIG. 6b. As in Fig. 6a except for outflow lifting condensation level $\mathcal{P}_0$, showing good correlation.

tance and on how far the inflow LCL differs from the asymptotic LCL given by the mean evaporation pressure scale $\overline{\Pi}_E$ is clear. Thus, we see that descent distance alone is insufficient to determine the total evaporation.

Over Venezuela we have only single station data which show the change in structure with the passage of a convective storm. Therefore, we shall not attempt to define an environment and apply the constant buoyancy model (Section 5c).

The Venezuelan storms showed a nearly wet adiabatic temperature structure (constant θ_{ES}) in the lowest 100–150 mb (Betts, 1976) with moister air near the surface with a higher θ_E but a lower θ_{ES}. From the "bulk" downdraft viewpoint this is at least consistent with descent in downdrafts with nearly constant Π_E and ρW_D until the air is slowed down close to the surface. Zipser (1977) has suggested an alternate explanation: that the cooler moister air near the surface came down in a more nearly saturated cloud-scale downdraft of higher θ_E, which undercuts a mesoscale downdraft which has higher θ_{ES} but is drier with resulting lower θ_E. The model trajectories in Miller and Betts (1977) also support this explanation. However, from the thermodynamic diagnostic viewpoint any air which finds itself close to the surface under precipitation will be brought closer to saturation at its wet-bulb temperature. This is being investigated further.

7. Conclusions

We have identified and explored the role of an evaporation pressure scale (Π_E) in determining the thermodynamic profiles within a moist downdraft. Π_E is a function of cloud-scale parameters: it increases with downdraft speed, and mean drop size, and decreases with increasing rainfall rate (see Fig. 1). From the theoretical viewpoint two special cases are illuminating. If Π_E is a constant, then the downdraft approaches an asymptotic state at constant relative humidity and constant pressure difference $\mathcal{P}$ to the LCL equal to Π_E, when the temperature path parallels a moist adiabat. Thus, the larger this evaporation pressure scale, the more unsaturated the downdraft becomes in its descent.

If, however, we assume the downdraft temperature path parallels the environment (so that downdraft buoyancy is constant), then the downdraft will move toward saturation or become more unsaturated depending on whether the environment is more or less stable than the moist adiabat. The trend toward (away from) saturation is associated with decreasing (increasing) Π_E, and by implication decreasing (increasing) downdraft speed. This analysis shows why downdrafts from the upper troposphere may not be possible. The theoretical section of this paper also showed how the downdraft thermodynamic paths can be constructed on a tephigram from a knowledge of Π_E and downdraft inflow properties (Fig. 3). The extension of the model to include entrainment into a downdraft was discussed briefly.

Cloud models used in cumulus parameterization could determine downdraft thermodynamic profiles by specifying a single, constant value of Π_E, although the dependence of Π_E on storm structure and variability requires much further investigation. Mass fluxes and inflow levels for the downdraft air must also be determined by other assumptions or closures.

The diagnostic section of this paper showed how profiles for Π_E families of downdraft parameters and profiles of the downdraft thermodynamic variables can be determined from downdraft inflow and outflow properties if additional model assumptions are made—particularly on the downdraft speed profile. Tropical data were used in illustration. Typical values of a vertically averaged $\overline{\Pi}_E$ were found to be in the range 20–100 mb. It was also found that this mean $\overline{\Pi}_E$ was not correlated to inflow properties (LCL or relative humidity) and may not, therefore, be simple to predict from large-scale variables. However, the pressure height to the LCL of the outflow, at least for this data, appears to bear a close relationship to $\overline{\Pi}_E$.

It is hoped that the use of this evaporation pressure scale may provide an organizing framework for the physical interpretation of downdrafts, whether derived diagnostically from soundings or budget studies or observed directly from aircraft or indirectly using doppler radars.

Acknowledgments. This work was supported by the National Science Foundation and the GATE Project Office under Grant ATM 77-15369, and by a Sloan Fellowship. We also owe much to discussion with the late Professor Frank Ludlam. M. Silva Dias acknowledges a scholarship from the Conselho Nacional de Desenvolvimento Cientifico e Technológico-CNPq-Brazil.

APPENDIX

The Lagrangian Water Conservation Equation

Derivation of Eq. (2) for a drop spectrum has been presented by Das (1969). It presents some national difficulty because different drop sizes have different fallspeeds, and the evaporation of drops changes the spectrum $n(r)$ expressed in terms of drop radius. For completeness we present a derivation here.

We may write the liquid water mass l in a volume element $\delta\tau$ as an integral per unit volume over drop number ν, mass $m(\nu)$, i.e.,

$$\rho l\delta\tau=\int_N m(\nu)\delta\tau d\nu, \tag{A1}$$

where N is the total number of drops per unit volume. The Eulerian flux form of the continuity of water substance is

$$\delta\tau\left\{\frac{\partial}{\partial t}(\rho q)+\nabla(\rho\mathbf{V}q)+\int_N\frac{\partial}{\partial t}[m(\nu)d\nu]+\nabla[(\mathbf{V}+\mathbf{V}_\nu)m(\nu)d\nu]\right\}=0, \tag{A2}$$

where $\mathbf{V}_\nu$ is the fallspeed relative to the air of the νth drop. (A2) can be transformed exactly into the Lagrangian form

$$\frac{D}{Dt}(\rho q\delta\tau)+\int_N\left(\frac{D}{Dt}\right)_\nu[m(\nu)\delta\tau d\nu]=0, \tag{A3}$$

where $(D/Dt)_\nu$ is a Lagrangian operator following the νth drop, by noting that $(D/Dt)_\nu(\delta\tau)=\delta\tau\nabla(\mathbf{V}+\mathbf{V}_\nu)$. Coalescence and breakup processes do not change the integral, which is the total mass of liquid in the elemental volume $\delta\tau$. However, evaporation changes the mass of each drop, so we may write the right-hand term as

$$\int_N\delta\tau d\nu\left(\frac{D}{Dt}\right)_\nu m(\nu)$$

and the left-hand term simplifies since $D/Dt(\rho\delta\tau)=0$ (conservation of mass). We obtain Eq. (2),

$$\rho\frac{Dq}{Dt}+\int_N d\nu\left(\frac{D}{Dt}\right)_\nu m(\nu)=0.$$

REFERENCES

Betts, A. K., 1976: The thermodynamic transformation of the tropical subcloud layer by precipitation and downdrafts. *J. Atmos. Sci.*, **33**, 1008–1020.

Brown, J. M., 1979: Mesoscale unsaturated downdrafts driven by rainfall evaporation: A numerical study. *J. Atmos. Sci.*, **36**, 313–338.

Byers, H. R., and R. R. Braham, 1949: *The Thunderstorm.* U.S. Dept. of Commerce, 287 pp.

Das, P., 1969: The thermodynamic equation in cumulus dynamics. *J. Atmos. Sci.*, **26**, 399–407.

——, and M. C. Subba Rao, 1972: The unsaturated downdraft. *Ind. J. Meteor. Geophys.*, **23**, 135–144.

Fujita, T., and H. R. Byers, 1977: Spearhead echo and downburst in the crash of an airliner. *Mon. Wea. Rev.*, **105**, 129–146.

——, and F. Caracena, 1977: An analysis of three weather related aircraft accidents. *Bull. Amer. Meteor. Soc.*, **58**, 1164–1181.

Haman, K., 1973: On the updraft-downdraft interaction in convective clouds. *Acta Geophys. Polonica*, **31**, 216–233.

Hookings, G. A., 1965: Precipitation maintained downdrafts. *J. Appl. Meteor.*, **4**, 190–195.

Houze, R. A., 1977: Structure and dynamics of a tropical squall-line system. *Mon. Wea. Rev.*, **105**, 1540–1567.

Johnson, R. H., 1976: The role of convective-scale precipitation downdrafts in cumulus and synoptic-scale interactions. *J. Atmos. Sci.*, **33**, 1890–1910.

Kamburova, P. L., and F. H. Ludlam, 1966: Rainfall evaporation in thunderstorm downdrafts. *Quart. J. Roy. Meteor. Soc.*, **92**, 510–518.

Kessler, E., 1969: *On the Distribution and Continuity of Water Substance in Atmospheric Circulation. Meteor. Monog.*, No. 32, Amer. Meteor. Soc., 84 pp.

Ludlam, F. H., 1963: *Severe Local Storms: A review. Meteor. Monog.*, No. 27, Amer. Meteor. Soc., 1–30.

——, 1979: *Clouds and Storms.* Pensylvania State University Press (to be published).

Manton, M. J., and W. R. Cotton, 1977: Formulation of approximate equations for modelling moist deep convection on the mesoscale. Atmos. Sci. Paper No. 266, Colorado State University, 62 pp.

Mason, B. J., 1971: *The Physics of Clouds*, 2nd ed. Clarendon Press, 671 pp.

Miller, M. J., and A. K. Betts, 1977: Travelling convective storms over Venezuela. *Mon. Wea. Rev.*, **105**, 833–848.

Nitta, T., 1977: Response of cumulus updraft and downdraft to GATE A/B-scale motion systems. *J. Atmos. Sci.*, **34**, 1163–1186.

Silva Dias, M. F., 1977: Diagnostic analysis of tropical cumulonimbus downdraft structure. Atmos. Sci. Paper No. 272, Colorado State University, 88 pp.

Yanai, M., S. Esbensen and J-H Chu, 1973: Determination of bulk properties of tropical cloud clusters from large-scale heat and moisture budgets. *J. Atmos. Sci.*, **30**, 611–627.

Zipser, E. J., 1969: The role of organized unsaturated convective downdrafts in the structure and decay of an equatorial disturbance. *J. Appl. Meteor.*, **8**, 799–814.

——, 1977: Mesoscale and cloud-scale downdrafts as distinct components in squall-line structure. *Mon. Wea. Rev.*, **105**, 1568–1589.